Mem. S.A.It. Vol. , 1

Memorie della

Numerical simulations of the quiet chromosphere

Jorrit Leenaarts[1]

Astronomical Institute - Utrecht University - PO Box 80 000 NL–3508 TA Utrecht, The Netherlands e-mail: j.leenaarts@uu.nl

Abstract. Numerical simulations of the solar chromosphere have become increasingly realistic over the past 5 years. However, many observed chromospheric structures and behavior are not reproduced. Current models do not show fibrils in Ca II 8542 Å, and neither reproduce the Ca II 8542 Å bisector. The emergent Hα line core intensity computed from the models show granulation instead of chromospheric shocks or fibrils. I discuss these deficiencies and speculate about what physics should be included to alleviate these shortcomings.

Key words. Sun: chromosphere, Methods: numerical

1. Introduction

The solar chromosphere is in many ways the most complicated and most interesting region of the solar atmosphere.

The chromosphere is the interface layer between the convection zone/photosphere and the corona where the value of the plasma β-parameter changes from larger to smaller than unity. Consequently, its overall character changes from a convective overshoot layer into a regime where the three-dimensional (3D) magnetic topology determines the structure. The chromosphere is convectively stable, so the dominant input of mechanical energy comes in the form of waves excited by granules and the buffeting of magnetic concentrations in the photosphere. It also absorbs radiation from both the photosphere (*e.g.,* H^-, Balmer-continuum) and the corona (He continua). Thermal conduction in the corona has a strong influence on the shape of the transition region, and hence of the upper chromosphere. The dominant chromospheric energy loss is through radiation in strong lines. Thus, a comprehensive model of the chromosphere cannot be made without modeling the underlying photosphere and upper convection zone and the overlying lower corona.

The wide range of pertinent physical processes require that a comprehensive description of the chromosphere needs to incorporate a careful combination of atomic and molecular physics, radiative transfer, MHD and plasma physics. This complicated physics requires numerical modeling.

From the above discussion I conclude that a "minimally satisfying self-consistent model" of the chromosphere should

- be time-dependent;
- be three-dimensional;
- model radiative heating and cooling;
- have a lower boundary in the convection zone, with a boundary condition that feeds enough energy into the simulation to main-

Send offprint requests to: J. Leenaarts

tain a the radiative energy loss at the solar effective temperature;
– have an upper boundary in the corona. If the model cannot self-consistently maintain a corona, it must provide enough energy flux to keep plasma near the boundary at coronal temperatures.

Within these constraints one can add features and physics to the model to increase its realism, while at the same time trying to keep the number of free parameters to a minimum.

The above list does not imply that models without those properties are somehow "bad models". To the contrary, simpler models are often instrumental in identifying and characterizing relevant physical processes. However, a thorough understanding of the chromosphere ultimately requires a self-consistent model that reproduces all observed chromospheric behavior.

2. Current status

The current state-of-the-art in self-consistent chromospheric modeling is the modeling performed with the radiation-magneto-hydrodynamics (RMHD) Oslo Stagger Code (OSC Hansteen 2004) and the MPI-parallelized Bifrost code currently under development (Gudiksen et al. 2010).

These codes are based on the methods pioneered by Nordlund (1982) in 3D convection simulations. They use the single-fluid MHD approach to model the solar gas and magnetic field. Radiative transfer in the photosphere and lower chromosphere is treated using multi-group opacity binning with scattering (Skartlien 2000) with typically 4 radiation bins. This multi-group scheme is not well suited to model the few strong chromospheric lines that cause the dominant radiative energy losses in the upper chromosphere. Therefore both codes employ parameterized radiative cooling in those lines in the upper chromosphere based on the detailed radiative transfer in a 1D dynamical chromospheric model (computed with the RADYN code, see *e.g.,* Carlsson & Stein 2002). Radiative losses in the corona are computed using an optically thin radiative loss function. Heat conduction parallel to the magnetic field is included. Two-dimensional simulations cannot maintain a corona by themselves and require additional heating at the upper boundary. Three-dimensional models however self-consistently maintain a corona by Joule heating.

Similar codes exist, such as Muram (Vögler et al. 2005), CO^{5}BOLD (Freytag et al. 2002; Wedemeyer et al. 2004) and RADMHD (Abbett 2008). However these codes so far do not support a corona (CO^{5}BOLD, Muram) or lack detailed treatment of the radiation field (RADMHD).

OSC has been used to study dynamic fibrils (DFs) by Hansteen et al. (2006) and De Pontieu et al. (2007a). They conclude that DFs are driven by magneto-acoustic shocks based on the similarity in dynamic behavior of wave-guided shocks in a 2D simulation and observations of DFs in the core of Hα. Their work has been extended to 3D in simulations by Martínez-Sykora et al. (2009b).

3D simulations of flux emergence from the convection zone through the chromosphere into the corona were performed by Martínez-Sykora et al. (2008, 2009a) A similar simulation showed the presence of Alfvénic waves with properties very much like what has been observed with the Hinode spacecraft (De Pontieu et al. 2007b).

For a good overview of 3D solar atmosphere modeling and post-processing in the form of 3D radiative transfer I refer the reader to Carlsson (2008, 2009) and references therein.

Despite the impressive progress that has been made in the last 5 years, many, often surprisingly basic properties of the chromosphere are not yet reproduced in the models. In the next section I discuss some of those observational facts and speculate about what is missing in the models.

3. Open questions and challenges

3.1. Lack of extended magnetic structure in Ca II 8542 Å

The first thing one notices in Ca II 8542 Å line-core images are the elongated structures delineating magnetic field lines around network regions. The NLTE Ca II 8542 Å computation from a snapshot of a 3D simulation of the chromosphere with OSC of Leenaarts et al. (2009) does, however, not show any such structures, despite the presence of a relatively strong magnetic field. Instead it shows the signature of oscillations and shocks, both in relatively field-free regions as in regions with stronger magnetic fields. Similar structures are observed in Ca II 8542 Å quiet regions away from the network. The lack of fibrils in the simulation is in my opinion the most pressing challenge models of the chromosphere currently face.

There can be many reasons for this lack. It might be that such fibrils require large-scale magnetic field configurations that do not fit in the typical size of the computational domain of $16 \times 16 \times 16$ Mm^3. It might be that the simulation cannot form fibrils due to a lack of grid resolution. Alternatively, fibril-like structures might exist in the models, but the lack of resolution inhibits mass loading of the fibrils, possibly due to too large numerical viscosity (see also Sec. 3.2). This lack of mass then translates into optically thin fibrils. Another possibility is that Ca II 8542 Å opacity in the fibrils is caused by physical processes currently not modeled in the simulations, for example non-equilibrium ionization or plasma effects that cannot be modeled within the MHD assumption.

3.2. Line broadening and bisector

The spatially averaged Ca II 8542 Å line profile computed in 3D NLTE from the same OSC snapshot shows a too narrow and too deep line core compared to observations (see Figs. 2 and 3 of Leenaarts et al. 2009). These calculations did not employ any non-physical microturbulence, and had a rather large grid cell size of $64 \times 64 \times 32$ km^3. The too narrow core was attributed to this lack of spatial resolution. Indeed, a newer simulation by Carlsson (private communication) with a cell size of $32 \times 32 \times 16$ km^3 shows a shallower and wider average Ca II 8542 Å core, but not yet as wide and shallow as observed. The increase in grid resolution causes an increase in amplitude of the velocity variations in the mid and upper chromosphere, and hence a widening of the average profile.

This result suggests that with even higher resolution the width of the line core might at least be qualitatively explained. However, the observed profile is at least partially formed in fibrils and as long as the models do not reproduce these the core width and depth remains not completely understood.

The low resolution simulation also did not reproduce the observed inverse C-shape of the Ca II 8542 Å line bisector. Similar results were obtained earlier by Uitenbroek (2006) who computed the NLTE line profiles from both a 3D simulation that did not extend into the corona and a dynamic 1D model. It would be interesting to see whether the bisector shape can be reproduced by high-resolution simulations, or that it is determined by phenomena currently not present in the simulations.

3.3. Lack of Hα opacity

The identification of DFs as magneto-acoustic shocks guided along magnetic field lines has been established based on the excellent agreement of dynamical properties observed in Hα with 2D simulations (Hansteen et al. 2006; De Pontieu et al. 2007a).

In a simulation with identical resolution and magnetic field configuration, Leenaarts et al. (2007) investigated the effect of non-equilibrium hydrogen ionization on the chromosphere. They found that the hydrogen $n = 2$ level populations and column densities are much higher in the simulated DFs than elsewhere in the chromosphere. This is consistent with the observations where DFs appear dark on top of a brighter, deeper formed background. However, a subsequent NLTE column-by-column radiative transfer computation employing non-equilibrium

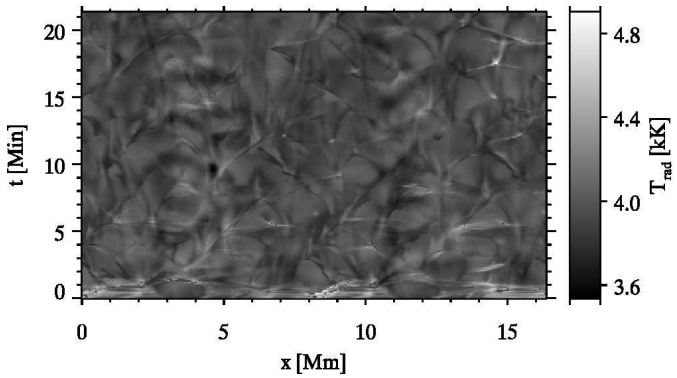

Fig. 1. Vertically emergent Hα line core intensity from a 2D radiation-MHD simulation with non-equilibrium hydrogen ionization taken into account. Startup effects are visible the first 3 minutes. There is a weak imprint of upward propagating shocks, superimposed on a slower-evolving pattern caused by granulation and reversed granulation. No parabolic outlines of DFs are present as in the observations (see Fig. 7 of De Pontieu et al. 2007a).

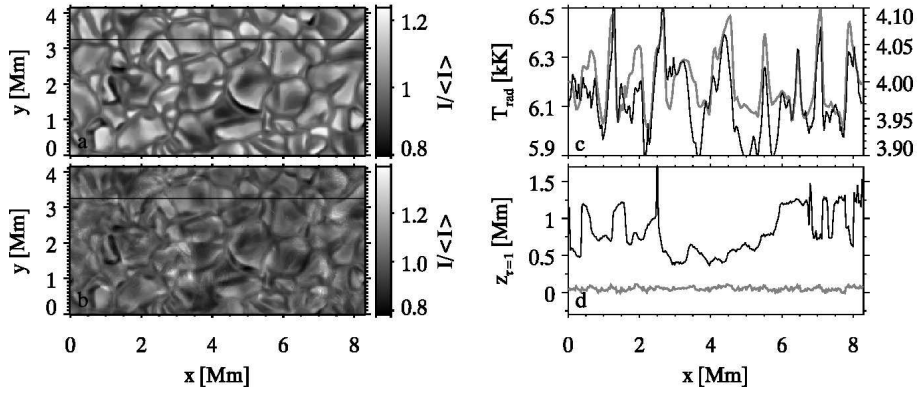

Fig. 2. Results of a NLTE radiative transfer computation of the Hα line from a 3D radiation-MHD simulation with an LTE equation of state. The black line in panels a and b indicates the cut shown in panel c and d. Panel a: vertically emergent intensity in the far blue wing; b: vertically emergent intensity at line center; c: vertically emergent intensity along the cut indicated in panels a and b for the blue wing (grey, left-hand scale) and line center (black, right hand scale); d: $\tau = 1$ height for the blue wing (grey) and line center (black).

temperatures and electron densities, but assuming statistical equilibrium for the hydrogen level-populations, showed that the upper chromosphere is transparent in the Hα line core in this simulation.

Fig. 1 shows the time-evolution of the vertically emergent Hα line center intensity. There are magnetic field concentrations at $x = 4$ Mm and $x = 12$ Mm along which DFs run up in the chromosphere. Their tops should appear as parabolic curves in this xt-slice, but instead the slice shows a slowly evolving pattern of granulation and reverse granulation. Superimposed on this pattern is a weak imprint of upward propagating shocks (the diagonal curves emanating from the magnetic field concentrations, for example the one starting at $(x, t) = (5.5, 10)$ Analysis of the contribution functions shows

that this imprint forms below 1 Mm, much lower than the typical height of DFs (see Fig. 16 of De Pontieu et al. 2007a).

Fig. 2 shows the results of a NLTE column-by-column radiative transfer computation of a snapshot of a 3D simulation of flux-emergence by Martínez-Sykora et al. (2008). This simulation used an LTE equation of state unlike the 2D simulation that used a more realistic non-equilibrium equation of state. Panels a and b show that the Hα line core shows granulation, even though its $\tau = 1$ height lies between 0.3 and 1.7 Mm (panel d). The line source function is strongly scattering and set in the upper photosphere, where it is sensitive to the temperature pattern of the granulation.

Both the 2D non-equilibrium simulation and the 3D LTE simulation show an Hα line center intensity pattern that is set in the upper photosphere, in stark contrast to the observations which show fibrilar structure in all but the quietest areas of the atmosphere. Even in such quiet areas the observations do not show granulation, but signatures of shockwaves instead (Rutten et al. 2008).

Some of the reasons that might cause the absence of fibrils in the simulated Ca II 8542 Å line core also apply here: too small computational domain, too low spatial resolution or the limitations of the MHD assumption. The 2D simulation necessarily had a rather simple magnetic field topology, which might inhibit the formation of fibrils and the mass loading of the upper chromosphere. The 3D simulation did not suffer from this, but it had lower resolution and did not model non-equilibrium ionization. High resolution 3D models with non-equilibrium hydrogen ionization might have a chromosphere that is optically thick in Hα.

Hydrogen line formation is however notoriously difficult to model. The non-equilibrium ionization of hydrogen does not only affect the electron density and temperature in the chromosphere, it also has a strong effect on hydrogen line formation. The standard NLTE line formation assumption of statistical equilibrium is not valid because of the slow collisional and radiative transition rates as compared to the hydrodynamical timescale. In addition at least the Lyman-α nd β lines need to be modeled with partial frequency redistribution (PRD) because of their strong influence on the Hα line. Both time-dependent radiative transfer and PRD effects were ignored in the results of Figs. 1 and 2. Inclusion of these effects might significantly increase the Hα opacity.

Thus, proper 3D modeling of the Hα line requires full time-dependent radiative transfer with PRD in tandem with the MHD evolution, a Herculean task that has not even been done in 1D hydrodynamic simulations. So far all 1D simulations perform radiative transfer in complete redistribution (Carlsson & Stein 2002; Rammacher & Ulmschneider 2003; Kašparová et al. 2009).

An easier way out is to perform the 3D radiation-MHD simulations with approximate non-equilibrium hydrogen ionization following the method developed by Sollum (1999) as was done in 2D by Leenaarts et al. (2007) in order to get reasonably accurate values for the electron density and temperature. One can then perform time-dependent radiative radiative transfer with PRD on a series of snapshots from the simulation to get the Hα line profiles. This separates the detailed radiative transfer from the MHD computation, which significantly reduces the difficulty of the problem. However, even with this simplification it remains a daunting task to accurately model Hα line formation in the dynamic chromosphere.

4. Summary & conclusions

Multidimensional radiation-MHD simulations of the solar chromosphere are becoming increasingly realistic. They have, amongst other things, been used to study dynamic fibrils, flux emergence and the propagation of Alfvénic waves into the corona.

The models yet fail to reproduce some observational facts:

- simulated Ca II 8542 Å core images do not show fibrils;
- the average simulated Ca II 8542 Å core is deeper and narrower than observed and its bisector not show the observed inverse C-shape;
- the simulated Hα line core shows granulation, both in 2D simulations with non-

equilibrium effects taken into accounts and in 3D with an LTE equation of state.

In order to reproduce these the models probably require higher resolution, larger computational domains, an improved treatment of radiation and non-equilibrium hydrogen ionization and inclusion of plasma effects. In order to model hydrogen transitions, in particular Hα, 3D NLTE time-dependent radiative transfer codes including PRD need to be developed.

Acknowledgements. J.L. acknowledges financial support by the European Commission through the SOLAIRE Network (MTRN-CT-2006-035484) and the Netherlands Organisation for Scientific Research (NWO).

References

Abbett, W. P. 2008, in Astronomical Society of the Pacific Conference Series, Vol. 383, Subsurface and Atmospheric Influences on Solar Activity, ed. R. Howe, R. W. Komm, K. S. Balasubramaniam, & G. J. D. Petrie , 327

Carlsson, M. 2008, Physica Scripta Volume T, 133, 014012

Carlsson, M. 2009, Memorie della Societa Astronomica Italiana, 80, 606

Carlsson, M. & Stein, R. F. 2002, ApJ, 572, 626

De Pontieu, B., Hansteen, V. H., Rouppe van der Voort, L., van Noort, M., & Carlsson, M. 2007a, ApJ, 655, 624

De Pontieu, B., McIntosh, S. W., Carlsson, M., et al. 2007b, Science, 318, 1574

Freytag, B., Steffen, M., & Dorch, B. 2002, Astronomische Nachrichten, 323, 213

Gudiksen, B. V., Carlsson, M., Hansteen, V., et al. 2010, A&A, in preparation

Hansteen, V. H. 2004, in IAU Symposium, ed. A. V. Stepanov, E. E. Benevolenskaya, & A. G. Kosovichev, 385–386

Hansteen, V. H., De Pontieu, B., Rouppe van der Voort, L., van Noort, M., & Carlsson, M. 2006, ApJ, 647, L73

Kašparová, J., Varady, M., Heinzel, P., Karlický, M., & Moravec, Z. 2009, A&A, 499, 923

Leenaarts, J., Carlsson, M., Hansteen, V., & Rouppe van der Voort, L. 2009, ApJ, 694, L128

Leenaarts, J., Carlsson, M., Hansteen, V., & Rutten, R. J. 2007, A&A, 473, 625

Martínez-Sykora, J., Hansteen, V., & Carlsson, M. 2008, ApJ, 679, 871

Martínez-Sykora, J., Hansteen, V., & Carlsson, M. 2009a, ApJ, 702, 129

Martínez-Sykora, J., Hansteen, V., DePontieu, B., & Carlsson, M. 2009b, ApJ, 701, 1569

Nordlund, A. 1982, A&A, 107, 1

Rammacher, W. & Ulmschneider, P. 2003, ApJ, 589, 988

Rutten, R. J., van Veelen, B., & Sütterlin, P. 2008, Sol. Phys., 28

Skartlien, R. 2000, ApJ, 536, 465

Sollum, E. 1999, Master's thesis, University of Oslo

Uitenbroek, H. 2006, ApJ, 639, 516

Vögler, A., Shelyag, S., Schüssler, M., et al. 2005, A&A, 429, 335

Wedemeyer, S., Freytag, B., Steffen, M., Ludwig, H.-G., & Holweger, H. 2004, A&A, 414, 1121